JOURNAL OF RESEARCH of the National Bureau of Standards—C. Engineering and Instrumentation
Vol. 72C, No. 2, April–June 1968

Calculation of Substitution Error in Barretters

Stephen Jarvis, Jr.,* and John W. Adams**

Institute for Basic Standards, National Bureau of Standards, Boulder, Colo. 80302

(January 22, 1968)

This paper describes a mathematical analysis for determining the value of the substitution error of a bolometer with a Wollaston-wire element (barretter). The analysis reflects all significant nonlinearities in the heat flow, including some not covered before, and includes all appreciable heat transport mechanisms simultaneously.

The values of substitution error thus obtained, in conjunction with efficiency data obtained by microwave techniques, will be very useful in extending power meter calibrations to frequency ranges where extremely accurate microcalorimeters are not available.

Key Words: Barretter, bolometer, microwave power measurements, substitution error.

1. Introduction

This paper describes a mathematical analysis for determining the value of the substitution error of a bolometer with a Wollaston-wire element (barretter). The analysis reflects all significant nonlinearities in the heat flow, including some not covered before, and includes all appreciable heat transport mechanisms simultaneously. The microwave current distribution has been measured in a scaled model and found to be approximately sinusoidal in shape with a current maximum in the middle of the wire. Input data are chosen so as to represent the operating bolometer characteristics as nearly as possible.

The values of substitution error thus obtained, in conjunction with efficiency data obtained by microwave techniques [1],[1] will be very useful in extending power meter calibrations to frequency ranges where extremely accurate microcalorimeters are not available. A method of measuring substitution error involves two distinct measurement techniques [1, 2], and since agreement is quite good between the value of substitution error thus measured and the value calculated from this analysis, the two provide a cross-check for each other.

2. Background

In the measurement of microwave and millimeter-wave power (hereafter referred to as rf power) by substitution techniques, any substitution error is of great concern. A common measurement technique is to replace a known amount of d-c power with an unknown amount of rf power in a bolometer. Unfortunately, the different current distributions generate different temperature fields which give the bolometer element slightly different values of total resistance for equal amounts of power. For balanced-bridge methods the resistance is maintained constant, which causes some non-equivalence of power. In this case Carlin and Sucher [3] defined substitution error as

$$E=\frac{W_{\mathrm{SUB}}-W_{\mathrm{rf}}}{W_{\mathrm{rf}}},$$

where W_{rf} is the rf power dissipated in the barretter element and W_{SUB} is the substituted d-c power which yields the same value of barretter resistance. Although a bolometer can be used to measure relative powers without calibration, it must be calibrated to measure absolute power. An accurate method of calibration is by the use of a microcalorimeter [2], in which the ratio of W_{SUB} to the net rf power flowing across an arbitrary plane W_{NET} into the bolometer is measured. This quantity is called the effective efficiency, $\eta_e=W_{\mathrm{SUB}}/W_{\mathrm{NET}}$. Another calibration method (for barretters only) is the impedance technique [1], in which the ratio of W_{rf} to W_{NET} is measured. This quantity is called the efficiency, $\eta=W_{\mathrm{rf}}/W_{\mathrm{NET}}$. By replacing W_{SUB} and W_{rf} in the equation for E, an equivalent form is given by

$$E=\frac{\eta_e-\eta}{\eta}.$$

*Radio Standards Laboratory, Consultant in Mathematics and Mathematics Group, NBS, Boulder, Colo. 80302.

**Radio Standards Laboratory, Microwave Circuit Standards, NBS Boulder, Colo. 80302.

[1] Figures in brackets indicate the literature references at the end of this paper.

This provides a way of measuring substitution error, but with the substantial limitation that in typical cases this necessitates subtracting two nearly equal numbers, and the relative uncertainty of the result is very large. Some results, comparisons, and comments will be given later.

Another equation derived from the previous ones is given by

$$W_{\text{NET}}=\frac{W_{\text{SUB}}}{\eta(1+E)}.$$

This form provides a method of measuring the net power from W_{SUB}, η, and E. The substituted d-c power is measured relatively easily, efficiency can be measured by the impedance technique (as mentioned previously), and now with the results of the analysis of this paper, substitution error can be calculated. For frequency ranges where microcalorimeters are not available, or for organizations to which they are not accessible, this provides an accurate means of calibrating barretters.

Previous work on determination of substitution error has been done by Carlin and Sucher [3], Weber [4], and Bleaney [5]. However, none of the previous workers attempted to solve the total heat-flow problem or to take into account all of the nonlinearities. Carlin and Sucher have determined an upper bound of substitution error from a combination of solutions to parts of the total problem. Weber has handled one nonlinearity in a solution to part of the problem.

3. Description of the Barretter

The actual barretter as shown in figure 1 can be represented by the model shown in figure 3. Partial justification for this is based on results of a model that used electric potential to represent temperature potential (fig. 2). These results showed that flush supports in a model yield negligible difference in potential from other common support structures. This is important, not only because flush supports give the simplest mathematical model, but also because there are large variations in the shapes and dimensions of support structures, even for the same models by the same manufacturer (fig. 4).

The rest of the justification for using the model shown in figure 3 becomes clear in the discussion of operation and different heat transport mechanisms that follows.

The barretter is a small-diameter, platinum wire of radius a and length l (fig. 3). It is supported at each end by a silver wire of larger diameter, and is normally immersed in air. Possible external, forced-convection currents are eliminated by a plastic shield of radius b which is nominally transparent to the electromagnetic fields.

For power measurements, this fine wire is usually heated with a d-c current to a particular value of resistance in the absence of rf fields, and then the d-c current is reduced to maintain the previous value of

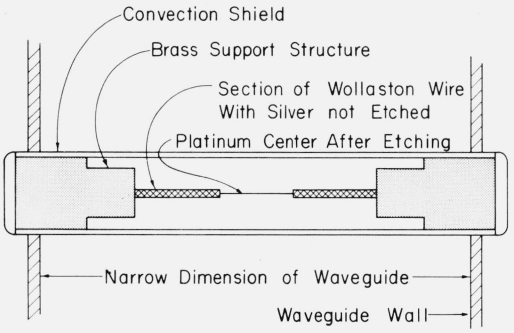

FIGURE 1. *Cross section of typical bolometer.*

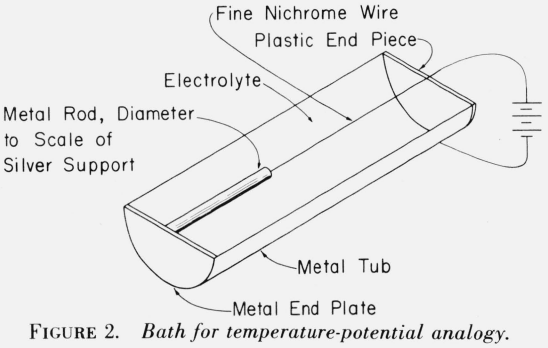

FIGURE 2. *Bath for temperature-potential analogy.*

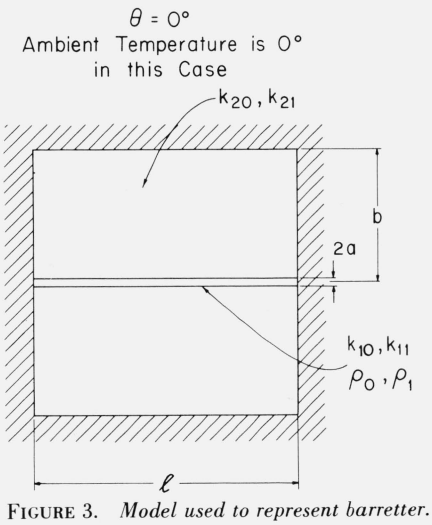

FIGURE 3. *Model used to represent barretter.*

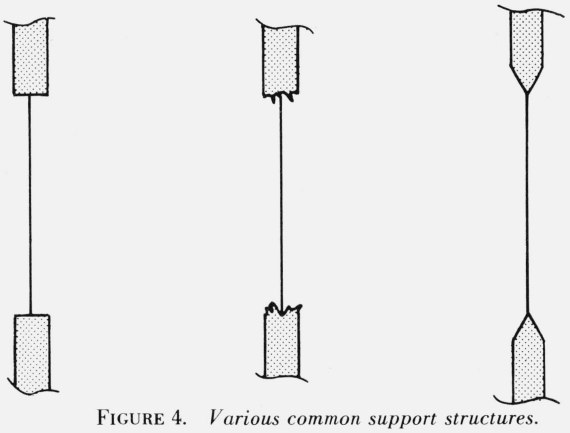

FIGURE 4. *Various common support structures.*

resistance when the rf field of frequency f is applied. The substituted d-c power is $(I_1^2 - I_2^2)R$, where I_1 is the d-c current without rf power, I_2 is the d-c current with rf power, and R is the value of resistance to which the barretter is biased. The substitution error is caused by the difference in temperature fields between the two heating conditions. The solution of these two temperature fields will then require the additional data concerning thermal properties of the wire and the surrounding fluid, usually air. The thermal conductivity of the wire, with its temperature coefficient, may be represented by $k_1 = k_{10} + k_{11}T$. Similarly the thermal conductivity of the fluid may be represented by $k_2 = k_{20} + k_{21}T$. The resistivity of the wire and the corresponding temperature coefficient may be represented by $\rho = \rho_0 + \rho_1 T$.

The previously mentioned parameters could all be input data; however, as is mentioned later, it is more judicious and accurate to arrive at some of these parameters from other measurements taken under operating conditions.

All heat-transfer mechanisms that can possibly act in a barretter will have to be considered and evaluated. Of conduction, convection and radiation, only conduction turns out to be significant. Radiation is negligible since surface area of the wire is so very small. Power radiated is given by

$$\rho = \sigma S F (T_2^4 - T_1^4),$$

where ρ is power in watts,
σ is the Stefan-Boltzman constant,
S is the surface area of the fine wire,
F is a surface emissivity factor and the T's are absolute temperatures in °K.

The diameter of the wire is of the order of magnitude 10^{-4} cm, and typical calculations show the radiated power to be less than 0.01 percent of the total power, even if the wire were at its melting temperature. Convection may also be shown to be negligible (0.01%) by evaluation of the Grashof number which is somewhat proportional to convective heat transport. This may also be confirmed by varying the orientation while measuring d-c power. The Grashof number is

$$N_{Gr} = \frac{\beta g \rho^2 L^3 (T_2 - T_1)}{\eta^2}$$

where β is the cubical expansion coefficient,
g is the gravitational constant,
ρ is the density,
L is the width of the gas space inside the plastic convection shield,
η is viscosity, and
T's are the absolute temperatures.

The Grashof number thus calculated for typical bolometers is less than 10; if it is less than 1000, convection may be considered negligible.

The only remaining heat transport mechanism, conduction, can be through both the fine wire and the air (or other fluid). The thermal conductivities of both media are functions of temperature over the rather wide temperature range for normal operation.

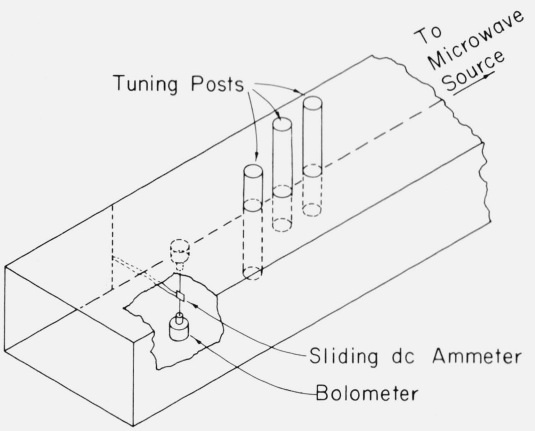

FIGURE 5. *8 × 16 in Scale model of waveguide bolometer for measuring rf current distribution in element.*

It is essential to consider the current distribution in the wire. The d-c current distribution is considered uniform both axially and radially. The rf current is essentially uniform radially, even to frequencies as high as 100 GHz (< 10% variation), primarily due to the smallness of the wire. The axial rf current distribution is of greater uncertainty, and has been investigated extensively with a scale model (fig. 5). Details are discussed in the following three paragraphs.

The measured values indicate a current maximum near the middle of the wire and in general a sinusoidal or parabolic shape. There is a frequency dependence on the amount of curvature. There is great variation in current magnitude but only slight variation in shape with respect to relative position of the shorting end-plate and with respect to position of tuning screws.

Some variation in the location of the current maximum may be introduced if the shorting end plate is tilted only a few degrees from perpendicular. The shape and size of the wire support structure cause variations in the current shape, but to a large extent, only insofar as the wire length itself is varied. An extreme case not encountered in most bolometers is when there is no support structure—the wire supported only by the wide walls. In this case the current distribution is nominally uniform, with great susceptibility to asymmetry introduced by varying angles in the shorting end plate.

The measured values seem to follow a sinusoidal distribution with wavelength greater than free-space wavelength and with some asymmetry (< 30° for common support structures). The sinusoidal distribution has been used by previous workers [3, 4, 5], but effects of asymmetry have not been previously considered. Further investigation is being considered, but for present calculations rf current is assumed to be sinusoidal with a free-space wavelength.

There are several pitfalls in determining three of the input parameters a, ρ_0, and ρ_1.

First, the radius a or diameter d cannot be measured directly with a microscope without bringing the objective lens destructively close to the barretter if sufficient magnification is used.

Second, the small diameter of the wire causes ρ_0 to vary from the bulk properties of the metal [6] since the wire diameter approaches the mean free path of an electron; ρ_1 does not vary this way [7, 8].

Third, a set of three equations with a, ρ_0, ρ_1 unknown is homogeneous and the determinant vanishes; it is possible to solve only for two of the unknowns in terms of the third.

The second circumstance indicates that if a value for one of these three unknowns must be assumed, assuming a value for ρ_1 causes the least uncertainty. The equation

$$R_i\pi a^2-\rho_0 l=\rho_1 T_i l,\ i=1,\ 2$$

can then be solved for a and ρ_0 if two sets of R and T are given; l can be measured accurately. One of the R and T sets is for room temperature while the other is for operating temperature. The average operating temperature is calculated by the computer program, as mentioned later.

4. Analysis

In this section, we give a description of the analysis used to obtain the substitution error and of the approximations involved. Details are given in appendix A, to which reference is frequently made.

Referring to the model shown in figure 3, the basic mathematical problem is to solve two distinct cases of the heat flow equation

$$\nabla\cdot(k_0+k_1T)\nabla T=S(r,\ x,\ T) \tag{1}$$

for the temperature field $T(r,\ x)$, where $(k_0,\ k_1)$ are conductivity coefficients (different for $r<a$, $r>a$) and S is the local power dissipation. (A–2, A–3)

In the first case, the temperature distribution T_{I} is generated by the source S_{I} (A–1) due to dissipation of the d-c current $\mathscr{I}_1$ flowing uniformly in the wire with resistivity linearly dependent on T.

In the second case, the temperature distribution T_{II} is generated by the source S_{II} (A–4) due to dissipation of a d-c current $\mathscr{I}_2$, as above, and also due to the time-average dissipation of an rf current (A–9a):

$$\mathscr{I}_R(x,\ t)=\mathscr{I}_{R0}z(x)\cos\omega t, \tag{2}$$

where $z(x)$, the current profile, is given, and the amplitude $\mathscr{I}_{R0}$ is an unknown constant.

Boundary conditions on the temperature field $T(r,\ x)$ in each case are:

$$T,_r(0,\ x)=T(b,\ x)=0,\qquad (0\leqslant x\leqslant l);$$

$$T(r,\ 0)=T(r,\ l)=0,\qquad (0\leqslant r\leqslant b);$$

$$\{T(r,\ x),\ T,_r(r,\ x)\} \tag{3}$$

continuous across $r=a$, $(0\leqslant x\leqslant l)$.

The rf current amplitude $\mathscr{I}_{R0}$ is to be determined by requiring that, given $\mathscr{I}_1$ and $\mathscr{I}_2$, the total wire resistance R_{hot} be the same in each case (A–20):

$$R_{\mathrm{hot}}=\frac{1}{\pi a^2}\int_0^l dx(\rho_0+\rho_1T(0,\ x)). \tag{4}$$

Because of the nonlinearities, the problem posed above is not tractable, and several simplifying assumptions are introduced which lead to a linear system of equations involving a single parameter, the mean axial temperature:

$$\overline{T}_{\mathrm{I}}=\frac{1}{l}\int_0^l dxT_{\mathrm{I}}(0,\ x). \tag{5}$$

The linear system is solved iteratively and converges rapidly.

Before making the simplifying assumptions, it is useful to introduce the "quasi-temperatures" (A–5):

$$\begin{aligned}G(r,\ x)&=T_{\mathrm{I}}(r,\ x)\left(1+\frac{1}{2}\frac{k_1}{k_0}T_{\mathrm{I}}(r,\ x)\right),\\ H(r,\ x)&=T_{\mathrm{II}}(r,\ x)\left(1+\frac{1}{2}\frac{k_1}{k_0}T_{\mathrm{II}}(r,\ x)\right),\\ g(r,\ x)&=H(r,\ x)-G(r,\ x).\end{aligned} \tag{6}$$

These quantities simplify the heat flow equations, since

$$\begin{aligned}\nabla\cdot(k_0+k_1T_{\mathrm{I}})\nabla T_{\mathrm{I}}&=k_0\nabla^2G,\\ \nabla\cdot(k_0+k_1T_{\mathrm{II}})\nabla T_{\mathrm{II}}&=k_0\nabla^2H.\end{aligned} \tag{7}$$

The interface conditions at $r=a$ are, of course, more complicated:

$$\left\{k_0G,_r,\ G\left(1+\tau\left(\frac{k_1}{k_0}G\right)\right)\right\} \tag{8}$$

are continuous across $r=a$, $(0\leqslant x\leqslant l)$, with identical conditions on H. Here $\tau(x)$ is the inverse function (A–7b):

$$G\left(1+\tau\left(\frac{k_1}{k_0}G\right)\right)=T_{\mathrm{I}}. \tag{9}$$

The three basic simplifying assumptions that are made are the following:

First, the difference function g is assumed small:

$$|g(r,\ x)|\ll|G(r,\ x)|. \tag{10}$$

This approximation appears to be adequately justified by the fact that computed values indicate $|g|<0.15|G|$ at worst, while the axial average $\bar{g}=0$. Neglecting

$\mathcal{O}(|g|^2)$, we obtain equations of the form (A–8a, A–11):

$$\nabla^2 G + A_1 G[1 + \varphi_1(G)] = A_2,$$

$$\nabla^2 g + A_3 g[1 + \varphi_2(G)] = \epsilon(x)$$

$$\cdot [\rho_0 + \rho_1 G(1 + \varphi_3(G))], \tag{11}$$

where the A_i are constants (different for $r > a$, $r < a$), the functions $\varphi_i(G)$ depend on $\tau\left(\frac{k_1}{k_0} G\right)$, and for cases studied, we have again $|\varphi_i(G)| < 0.15$.

The function $\epsilon(x)$ depends on the difference in current flows in the d-c and rf cases. The second (nonlinear) interface condition is (A–14)

$$|G(1 + \varphi_4(G))|_{a^-}^{a^+} = 0,$$

$$|g(1 + \varphi_5(G))|_{a^-}^{a^+} = 0, \tag{12}$$

with $\varphi_i(G)$ as above.

The second simplifying assumption is that for $0 \leq r < a$, we may put

$$\varphi_i(G) = \varphi_i(\overline{G(0, x)}) \tag{13}$$

using the axial average, while for $r > a$, we may put

$$\varphi_i(G) = \varphi_i(G^*) \tag{14}$$

where G^* satisfies the interface condition in the mean

$$G^*(1 + \varphi_4(G^*)) = \overline{G}(1 + \varphi_4(\overline{G})). \tag{15}$$

This approximation makes use of the expected flatness of the temperature distribution in x, and is clearly better for large l/b. Numerical tests indicated the results were very insensitive to the choice of $\overline{G}$; a 5 percent change in $\overline{G}$ gave a 0.06 percent change in E in a typical case.

The third simplifying assumption, used indirectly above, is that we may put

$$G(r, x) = G(0, x) \tag{16}$$

in the source term for g, $(r \leq a)$. This is readily justified by the extremely small radial temperature drop in the wire.

With these simplifications, the linear equations with parameter $\overline{G}$ in (g, G) (A–12, A–13, A–17, A–18) are readily solved in terms of cylinder functions. With the same simplifying assumptions, we find the balanced bridge requirement (A–21):

$$\overline{g(0, x)} = 0 \tag{17}$$

which determines the unknown rf current amplitude $\mathcal{I}_{R0}$ implicit in $\epsilon(x)$.

After iteration to determine the parameter $\overline{G}$, the required power levels W_{SUB} and W_{rf}, the substitution error E (A–27), and the temperature distributions $T_{\text{I}}(0, x)$ and $\Delta T \equiv T_{\text{II}}(0, x) - T_{\text{I}}(0, x)$ (A–34a, A–34b) are readily found by numerical integrations involving $G(0, x)$ and the rf current profile $z(x)$.

Details of the computer programs are available from the authors. Further details for the sinusoidal rf current distribution are given in (A–37, A–38, A–39).

5. Uncertainties

With given input data, the analysis and computation described in the previous section is believed to yield a substitution error which is correct for the cases studied to within a few percent, though it has not been possible to construct an error bound.

An evaluation of the total differential reflecting the uncertainties of all the input data would seem to offer a limit of uncertainty to the calculated value of substitution error, so that one concerned with applying this technique would have sufficient justification for doing so. This figure is nominally 20 to 25 percent, which is quite adequate for the typically small values of substitution error.

Unfortunately the shape of the rf current distribution (assumed sinusoidal with a free space wavelength and with a current maximum in the middle) is known no better than it can be measured with a scale model. Uncertainties due to variation of wavelength and shift in position of current maximum are partially reflected in this total differential; phase shift variations cause only 0.2–0.3 percent decrease in substitution error, and are included in the above uncertainty, but the uncertainty as to wavelength could cause 10 to 40 percent change either way and is in addition to the above uncertainty. Even this is just a best-judgment estimate.

This degradation could be substantially reduced if a sound theoretical analysis of the current distribution in the barretter were available. Since none is, further investigation is certainly in order.

As to the input data, R_{cold} and R_{hot} may be measured quite accurately, while only two of the four quantities ρ_0, a, R_{cold} and R_{hot} are independent. First, the following relation must hold:

$$R_{\text{cold}} = \frac{\rho_0 l}{\pi a^2}. \tag{18}$$

A second relation results as follows: Given the parameters a and $x_i = \{R_{\text{cold}}, \rho_1, k_{ij}, b, l, \mathcal{I}_1^2, \mathcal{I}_2^2, f, \tan \varphi\}$ the temperature field $T(x, o)$ is determined in the wire, as is the heated wire resistance R

$$R = \frac{l}{\pi a^2} (\rho_0 + \rho_1 \overline{T(x, 0)})$$

$$= R(a; x_i) \tag{19}$$

and a substitution error is determined

$$E = \mathcal{E}(a; x_i). \tag{20}$$

An iteration is made to find a^* such that

$$R(a^*; x_i) = R_{\text{hot}} \tag{21}$$

which is the required second relation. Then also

$$E=\mathscr{E}(a^*;\ x_i) \tag{22}$$

is the proper substitution error.

These forms are also used to determine the effect on E of small uncertainties in the data x_i. From small changes in $(x_i,\ a)$, we compute the partial derivative approximations:

$$\left\{\frac{\partial\mathscr{E}}{\partial a},\ \frac{\partial R}{\partial a},\ \frac{\partial\mathscr{E}}{\partial x_i},\ \frac{\partial R}{\partial x_i}\right\}. \tag{23}$$

With the bridge balanced

$$\delta R_{\text{hot}}=\frac{\partial R}{\partial\alpha}\,\delta\alpha+\frac{\partial R}{\partial x_i}\,\delta x_i=0 \tag{24}$$

while

$$\delta E=\frac{\partial\mathscr{E}}{\partial\alpha}\,\delta\alpha+\frac{\partial R}{\partial x_i}\,\delta x_i. \tag{25}$$

Then

$$\delta E=\delta x_i\left\{\frac{\partial\mathscr{E}}{\partial x_i}-\frac{\partial\mathscr{E}}{\partial a}\frac{\dfrac{\partial R}{\partial x_i}}{\dfrac{\partial R}{\partial a}}\right\} \tag{26}$$

gives the error in E due to small input error δx_i.

6. Results, Comparisons, and Evaluation

Values of substitution error have been calculated for several common barretters and where possible comparisons are made with some measured values (see table 1). Although the agreement is reassuring, the uncertainty in the measurement makes the comparison inconclusive in itself.

A number of variations of input data lead to several interesting observations concerning the calculated values of substitution error.

Based on calculated results which use sinusoidal current distribution with free-space wavelength, substitution error varies approximately as the square of the frequency.

The effect of asymmetry in the current distribution (induced by asymmetries in the physical structure) is to slightly reduce the substitution error, typically of the order of magnitude of 0.1 to 0.3 percent.

The use of helium, a gas with higher thermal conductivity than air, greatly increases the power handling capacity of the barretter. It also increases the heat "coupling" to the surroundings and thus reduces the substitution error approximately 10 percent. The same effect is obtained (but without increasing the power handling capacity) by increasing the bias current (e.g., so that the resistance increases from 200 to 267 Ω).

A change in rf power level causes virtually no change in substitution error.

The nonlinearity due to the temperature dependence of the thermal conductivity of the air causes an approximate 15 percent increase in substitution error over what would have occurred if that nonlinearity had not been present. The temperature dependence of the thermal conductivity of the metallic element causes only slight variation ($\approx 1\%$) in substitution error as only about 5 percent of the heat escapes the element by metallic conduction.

TABLE 1. *Comparison of measured and calculated values of substitution error*

Freq (GHz)	NBS barretter unit	Effective efficiency (η_e)	Efficiency (η)	No. of meas.	Measured substitution error $E=\frac{\eta_e-\eta}{\eta}$	Calculated substitution error
8.2	18	0.9920 ± 0.002	0.9906 ± 0.005	12	0.0014	0.0020
12.2	23	.9709 ± 0.002	.9644 ± 0.005	3	.0067	.0056

It is also of interest to compare results with those of previous workers, in particular Carlin and Sucher [3]. Although they obtained an upper bound for substitution error, and this upper bound is typically 20–25 percent higher than our calculated results, a closer examination of their work points to a flaw in one of their conclusions, namely that nonlinearities have little effect in these cases. The margin of safety in their upper limit comes from the fact that they solve two related linear problems, calculate the substitution error for each case and add the results together to obtain a safe upper limit. It happens that both of these related problems resemble the real problem, their equation (15), quite closely, and the results of their equation (15) should be a good solution to the linear approximation to the real problem. The corresponding results of equation (15) are about 40 percent lower than our results in most typical cases; this indicates the magnitude of the error made in assuming that nonlinearities can be neglected.

Appendix A. Analysis

A wire of radius a and length l terminates on metallic surfaces at $z=0$ and $z=l$, the whole enclosed in a shield of inner radius b, as shown in figure 3. The wire is heated by current sources uniform in r, $(0\leqslant r\leqslant a)$, and the temperature T above ambient is assumed to vanish on the shield $r=b$, $(0\leqslant x\leqslant l)$ and on the end surfaces $z=(0,\ l)$, $(0\leqslant r\leqslant b)$.

Let T_1 be the temperature field in the d-c-only case, in which the source strength S_1 in the wire due to d-c current $\mathscr{I}_1$ is

$$S_1=\mathscr{I}_1^2(\bar{\rho}_0+\bar{\rho}_1 T_1) \tag{A-1}$$

where $(\bar{\rho}_0, \bar{\rho}_1) \equiv (\rho_0/A^2, \rho_1/A^2)$ and A is the cross-sectional area of the wire.

The heat flow vector is

$$q_1 = -(k_{i0} + k_{i1} T_1) \nabla T_1 \tag{A-2}$$

and governing equation for heat flow is

$$\nabla \cdot q_1 = S_1 \tag{A-3}$$

with subscript i referring to $0 \leq r < a$ and $a < r \leq b$ (fig. 1).

Let T_{II} be the temperature field in the rf-substitution case. The source strength $S_{II}(x)$ is taken to be a time average due to a d-c current $\mathscr{I}_2$ and an rf current $\mathscr{I}_R(x, t)$:

$$S_{II} = \langle [\mathscr{I}_2 + \mathscr{I}_R(x, t)]^2 \rangle (\bar{\rho}_0 + \bar{\rho}_1 T_{II}). \tag{A-4}$$

Equations analogous to (A-2, A-3) hold for the heat flow in this case.

The fields (T_1, T_{II}) and the heat flow vectors (q_1, q_{II}) are to be continuous across $r = a (0 \leq x \leq l)$.

Let us introduce new variables

$$\begin{aligned} G(r, x) &\equiv T_1 \left(1 + \frac{1}{2} r_i T_1\right) \\ H(r, x) &\equiv T_{II} \left(1 + \frac{1}{2} r_i T_{II}\right) \\ g(r, x) &\equiv H(r, x) - G(r, x), \end{aligned} \tag{A-5}$$

where

$$r_i \equiv k_{i1}/k_{i0}, \tag{A-6}$$

so that the definitions differ in the regions $r \gtrless a$. The relations in (A-5) may be inverted to give, e.g.:

$$T_1 = G(1 + \tau(r_i G)), \tag{A-7a}$$

$$\tau(x) \equiv \frac{-\frac{1}{2} x}{\left[\frac{1}{2} + \sqrt{\frac{1}{4} + \frac{1}{2} x}\right]^2} \tag{A-7b}$$

In terms of the Laplacian

$$\mathscr{L} \equiv \frac{1}{r} \frac{\partial}{\partial r} r \frac{\partial}{\partial r} + \frac{\partial^2}{\partial x^2},$$

$$k_{i0} \mathscr{L} \begin{bmatrix} G \\ H \end{bmatrix} = - \begin{bmatrix} \mathscr{I}_1^2 \delta_{i1} [\bar{\rho}_0 + \bar{\rho}_1 G(1 + \tau(r_1 G))] \\ \delta_{i1} \langle (\mathscr{I}_2 + \mathscr{I}_R(x, t))^2 \rangle [\bar{\rho}_0 + \bar{\rho}_1 H(1 + \tau(r_1 H))] \end{bmatrix}, \tag{A-8a, A-8b}$$

and in the region $r > a$, $(i = 2)$ Laplace's equation holds exactly. This is the critical region for heat loss.

We shall suppose the form of the rf-wave is given, but its amplitude $\mathscr{I}_{R0}$ is determined (for given $\mathscr{I}_1$, $\mathscr{I}_2$) to balance the bridge after substitution

$$\mathscr{I}_R(x, t) = \mathscr{I}_{R0} z(x) \cos \omega t. \tag{A-9a}$$

Then taking time average

$$\langle [\mathscr{I}_2 + \mathscr{I}_{R0} z(x) \cos \omega t]^2 \rangle = \mathscr{I}_2^2 + \frac{1}{2} \mathscr{I}_{R0}^2 z^2(x)$$

Let $\overline{(\quad)}$ denote the average on $(0, l)$ and define

$$z_1(x) = \frac{z^2(x)}{\overline{z^2(x)}} - 1, \qquad \overline{z_1(x)} = 0, \tag{A-9b}$$

so that

$$\mathscr{I}_2^2 + \frac{1}{2} \mathscr{I}_{R0}^2 z^2(x) = \mathscr{I}_2^2 + \frac{1}{2} \mathscr{I}_{R0}^2 \overline{z^2(x)} (1 + z_1(x)). \tag{A-9c}$$

In the long wave-length limit, $z^2(x)$ is a constant, $z_1(x) = 0$, so that if $\mathscr{I}_2^2 + \frac{1}{2} \mathscr{I}_{R0}^2 \overline{z^2(x)} = \mathscr{I}_1^2$, the sources S_1 and S_{II} are identical, so are the fields T_1, T_{II}, and there is no substitution error. We shall assume then that

$$\frac{1}{2} \mathscr{I}_{R0}^2 \overline{z^2(x)} D \mathscr{I}_1^2 - \mathscr{I}_2^2 + I^2, \tag{A-9d}$$

and thus that

$$S_{II} = [\mathscr{I}_2^2 + (\mathscr{I}_1^2 - \mathscr{I}_2^2 + I^2)(1 + z_1(x))] (\bar{\rho}_0 + \bar{\rho}_1 T_{II}), \tag{A-9e}$$

where $I^2/(\mathscr{I}_1^2 - \mathscr{I}_2^2)$ and $z_1(x)$ are assumed small compared with unity. We must expect $g(r, x)$ to be small also when $I^2/(\mathscr{I}_1^2 - \mathscr{I}_2^2)$ and $z_1(x)$ are small, and we linearize (A-8b) accordingly in g:

$$k_{i0} \mathscr{L} g = -\delta_{i1} [\mathscr{I}_1^2 B g + BC g + AC],$$

where

$$\begin{aligned} A &= \bar{\rho}_0 + \bar{\rho}_1 G(1 + \tau(r_1 G)) \\ B &= \bar{\rho}_1 (1 + \tau(r_1 G + r_1 G \tau'(r_1 G)) \\ C &= I^2 + (\mathscr{I}_1^2 - \mathscr{I}_2^2) z_1(x) + \mathscr{O}(I^2 z_1(x)). \end{aligned} \tag{A-10}$$

Now C is assumed small by virtue of $I^2/(\mathscr{I}_1^2-\mathscr{I}_2^2)$ and $z_1(x)$ being small, so that

$$BCg \ll \mathscr{I}_1^2 Bg.$$

Also since

$$\bar{\rho}_1 g \ll \bar{\rho}_0 + \bar{\rho}_1 G,$$

$$BCg \ll AC.$$

Thus we can neglect the second source term. We shall also neglect $\mathcal{O}(I^2 z_1(x))$ in C. Then we have

$$k_{i0}\mathscr{L}g = -\delta_{i1}\{g\mathscr{I}^2\bar{\rho}_1(1+\tau(r_1G) + r_1G\tau'(r_1G)) + [\bar{\rho}_0+\bar{\rho}_1G(1+\tau(r_1G))]\cdot [I^2+(\mathscr{I}_1^2-\mathscr{I}_2^2)z_1(x)]\} \quad \text{(A–11)}$$

We shall deal only with G(A–8) and g(A–11) to which must be appended boundary conditions:

$$\underline{r=0}: \frac{\partial G}{\partial r} = \frac{\partial g}{\partial r} = 0, \ (0 \leq x \leq l);$$

$$\underline{r=b}: G = g = 0, \ (0 \leq x \leq l);$$

$$\underline{x=0,\ l}: G = g = 0, \ (0 \leq r \leq b); \quad \text{(A–12)}$$

while the interface continuity conditions become

$$\underline{r=a}: \left| k_{i0}\frac{\partial G}{\partial r}\right|_{a^-}^{a^+} = 0,$$

$$\left| k_{i0}\frac{\partial g}{\partial r}\right|_{a^-}^{a^+} = 0, \quad \text{(A–13)}$$

for continuity of heat flow, and

$$\underline{r=a}: |G(1+\tau(r_iG))|_{a^-}^{a^+} = 0,$$

$$|g(1+\tau(r_iG)+r_iG\tau'(r_iG))|_{a^-}^{a^+} = 0, \quad \text{(A–14)}$$

where we have again used $|g| \ll |G|$ in the second condition in (A–14).

Now even in the region of the wire where the temperatures are highest, $\tau(r_1G) \approx 0.1$, so that the nonlinearity is small. Furthermore, because of the high conductivity of the wire compared to the air, the radial temperature gradient in the wire is negligible, and

$$G(r, x) \doteq G(0, x) \quad \text{(A–15)}$$

inside the wire.

The equations are still nonlinear in a way preventing the easy use of linear methods of solution. Extending the assumption that $\tau(r_iG)$ is only a small correction at worst, we assume that the average axial value of G may be used to evaluate $\tau(r_iG)$:

$$\tau(r_iG) \doteq \tau(r_i\bar{G}) \quad \text{(A–16)}$$

Then we shall use the differential equations

$$\begin{cases} k_{i0}\mathscr{L}G + \mathscr{I}_1^2\bar{\rho}_1(1+\tau_1)\delta_{i1}G = -\mathscr{I}_1^2\bar{\rho}_0\delta_{i1} \\ k_{i0}\mathscr{L}g + \mathscr{I}_1^2\bar{\rho}_1(1+\tau_2)\delta_{i1}g \end{cases}$$

$$= -[I^2 + (\mathscr{I}_1^2-\mathscr{I}_2^2)z_1(x)] \cdot [\bar{\rho}_0+\bar{\rho}_1G(x, 0)(1+\tau_1)]\delta_{i1} \quad \text{(A–17)}$$

where $\tau_1 = \tau(r_1\bar{G})$, $\tau_2 = \tau_1 + r_1\bar{G}\tau'(r_1\bar{G})$.

On $r=a$, we have the interface condition:

$$\underline{r=a}\begin{cases} G(a^-, x) = G(a^+, x)\sigma_1 \\ g(a^-, x) = g(a^+, x)\sigma_2, \end{cases} \quad \text{(A–18)}$$

where

$$\sigma_1 = \frac{1+\tau(r_2G^*)}{1+\tau_1}$$

$$\sigma_2 = \frac{1+\tau(r_2G^*)+r_2G^*\tau'(r_2^2G^*)}{1+\tau_2}$$

where G^* is the number which gives continuity of temperature at $r=a^+$ in the mean by (A–7a):

$$G^*(1+\tau(r_2G^*)) = \bar{G}(1+\tau(r_1\bar{G})). \quad \text{(A–19)}$$

The system of equations we solve then, (A–17), subject to conditions (A–18, A–13, A–12), are linear when $\bar{G}$ is given. From the solution, a new $\bar{G}$ is computed, and the solution iterated to make $\bar{G}$ stationary. With a reasonable guess, say only 25 percent off, five iterations brought $\bar{G}$ to within 1 percent.

No attempt has been made to bound the uncertainty of the substitution error due to the assumptions made. Possibly a better choice for the constant $\bar{G}$ than that given in (A–16) might be made. If a 5 percent increase in $\bar{G}$ is used to compute the (τ_i, σ_i), the substitution error changes by 0.06 percent in a typical case. The approximation is clearly better for large l/b, for which the temperature profile is flat for most of the wire length.

The constant I in the source of (A–17) for g is determined by the requirement that the total bolometer element resistance be unchanged when the d-c current $\mathscr{I}_1$ is replaced by the current $\langle(\mathscr{I}_2+\mathscr{I}_R(x, t))\rangle$. Equating these resistances:

$$\int_0^l dx[\bar{\rho}_0+\bar{\rho}_1G(0, x_1)(1+\tau(r_1G(0, x)))] = \int_0^l dx[\bar{\rho}_0+\bar{\rho}_1H(0, x)(1+\tau(r_1H(0, x)))] \quad \text{(A–20)}$$

Expanding H to 1st order in g, and again assuming $G(0, x)$ is flat enough to be replaced by its average in $\tau(r_1 G)$, we find

$$\int_0^l dx g(0, x) = 0; \tag{A-21}$$

for the balanced bridge this relation determines I in (A-17).

When no rf power is introduced, the d-c power developed in the bolometer element is

$$W_{DC1} = \pi a^2 \mathscr{I}_1^2 \int_0^l dx [\bar{\rho}_0 + \bar{\rho}_1 G(0, x)(1 + \tau(r_1 G))] \tag{A-22}$$

When the d-c current is reduced to $\mathscr{I}_2$ and rf current is added to rebalance the bridge, the total power developed is

$$W_{TOT} = \pi a^2 \int_0^l dx [\mathscr{I}_2^2 + \tfrac{1}{2} \mathscr{I}_{R0}^2 z^2(x)] \cdot [\bar{\rho}_0 + \bar{\rho}_1 H(0, x)(1 + \tau(r_1 H))] \tag{A-23}$$

$$\equiv W_{DC2} + W_{rf}$$

where by virtue of (A-20),

$$W_{DC2} = \zeta^2 W_{DC1}, \qquad \zeta \equiv \mathscr{I}_2 / \mathscr{I}_1. \tag{A-24}$$

The substituted power is defined as

$$W_{SUB} = W_{DC1} - W_{DC2} = (1 - \zeta^2) W_{DC1} \tag{A-25}$$

The change in power developed ΔW (with A, B, C as before (A-10), and using the same approximations and the bridge balance relation (A-21)) is found to be:

$$\Delta W = W_{TOT} - W_{DC1} = W_{rf} - W_{SUB}$$

$$= \pi a^2 \int_0^l dx (AC + \mathscr{I}_1^2 Bg)$$

$$= \pi a^2 \int_0^l dx [\bar{\rho}_0 + \bar{\rho}_1 G(0, x)(1 + \tau_1)] \cdot [I^2 + \mathscr{I}_1^2 - \mathscr{I}_2^2 z_1(x)]. \tag{A-26}$$

Then the substitution error is

$$E = -\frac{\Delta W}{W_{rf}} = -\frac{-\frac{\Delta W}{W_{SUB}}}{1 + \frac{\Delta W}{W_{SUB}}}. \tag{A-27}$$

Let $\chi^{(j)}(x, r; \xi, \eta)$ be Green's functions for the systems (A-17) with the superscript ($j = 1, 2$) referring to (τ_1, σ_1) for G and (τ_2, σ_2) for g. The Green's function is symmetric in (x, ξ). Let:

$$G^{(j)}(x) = -(1 + \tau_j)\bar{\rho}_1 \mathscr{I}_1^2 \int_0^l d\xi \int_0^a d\eta \eta \chi^{(j)}(x, 0; \xi, \eta). \tag{A-28}$$

We define the numbers

$$A_{1,2} = \int_0^l dx (1 + G^{(1)}(x)) \begin{bmatrix} 1 \\ G^{(2)}(x) \end{bmatrix},$$

$$B_{1,2} = \int_0^l dx (1 + G^{(1)}(x)) z_1(x) \begin{bmatrix} 1 \\ G^{(2)}(x) \end{bmatrix}. \tag{A-29}$$

The bridge balance condition (A-21) leads to

$$\frac{I^2}{\mathscr{I}_1^2 - \mathscr{I}_2^2} = -\frac{B_2}{A_2}. \tag{A-30}$$

In terms of the (A_i, B_i), the power terms can be written as

$$W_{SUB} = (1 - \rho^2) \pi a^2 \bar{\rho}_0 \mathscr{I}_1^2 A_1, \tag{A-31}$$

$$\Delta W = \pi a^2 \bar{\rho}_0 \mathscr{I}_1^2 (1 - \rho^2) \left[\frac{I^2}{\mathscr{I}_1^2 - \mathscr{I}_2^2} A_1 + B_1 \right], \tag{A-32}$$

so that the substitution error is

$$E = \frac{A_1 B_2 - B_1 A_2}{A_1 A_2} \left[1 - \frac{A_1 B_2 - B_1 A_2}{A_1 A_2} \right]^{-1}. \tag{A-33}$$

The axial temperature distributions themselves are found from

$$T_I(x) = \frac{\bar{\rho}_0}{\bar{\rho}_1} \sum_{n=1}^{\infty}{}^* \varphi_n^{(1)} \sin \frac{n\pi x}{l} \tag{A-34a}$$

$$\Delta T(x) \equiv T_{II}(x) - T_I(x) = \frac{\pi \bar{\rho}_0}{l \bar{\rho}_1} \sum_{n=1}^{\infty} \psi_n^{(2)} \sin \frac{n\pi x}{l} \cdot \left(1 - \frac{\zeta^2}{2}\right) \tag{A-34b}$$

where Σ^* is a sum over odd n only, the coefficients $\varphi_n^{(i)}$ are given in Appendix B, and

$$\psi_n^{(2)} = n\varphi_n^{(2)} \left[\frac{I^2}{\mathscr{I}_1^2 - \mathscr{I}_2^2} A_{3n} + B_{3n} \right] = \frac{n\varphi_n^{(2)}}{A_2} (B_{3n} A_2 - A_{3n} B_2), \tag{A-35}$$

$$\begin{bmatrix} A_{3n} \\ B_{3n} \end{bmatrix} \equiv \int_0^l dx (1 + G^{(1)}(x)) \sin \frac{n\pi x}{l} \begin{bmatrix} 1 \\ z_1(x) \end{bmatrix}. \tag{A-36}$$

Our primary concern is with a sinusoidal current distribution

$$z(x) = \cos \left[kl \left(\frac{1}{2} - \frac{x}{l} \right) + \varphi \right] \tag{A-37}$$

from which we compute $z_1(x)$ by (A-9a).

Then

$$z^2(x)=\cos^2\varphi\cos^2 kl\left(\frac{1}{2}-\frac{x}{l}\right)+\sin^2\varphi\sin^2 kl\left(\frac{1}{2}-\frac{x}{l}\right)+\mathscr{A}(x), \qquad \text{(A-38)}$$

where

$$\mathscr{A}(x)\equiv-\frac{1}{2}\sin 2\varphi\sin 2kl\left(\frac{1}{2}-\frac{x}{l}\right)$$

does not contribute since it is anti-symmetric on $(0, l)$ while $G^{(i)}(x)$ are symmetric.

We find, averaging and noting $\overline{\mathscr{A}(x)}=0$.

$$\overline{z^2(x)}=\cos^2\varphi\left[\frac{1}{2}+\frac{\sin\frac{kl}{2}\cos\frac{kl}{2}}{kl}\right]+\sin^2\varphi\left[\frac{1}{2}-\frac{\sin\frac{kl}{2}\cos\frac{kl}{2}}{kl}\right]. \qquad \text{(A-39)}$$

We obtain $z_1(x)$ from (A-38, A-39) using (A-9b).

In Appendix B, details of the calculation of the $G^{(i)}(x)$ by Fourier series, description of a program used to compute the (A_i, B_i) and the temperature distributions are presented.

Appendix B. Green's Function

We are to determine the Green's function $\chi^{(j)}(x, r; \xi, \eta)$ satisfying the system

$$k_{i0}\mathscr{L}\chi^{(j)}+\mathscr{I}_1^2\bar{\rho}_1(1+\tau_j)\chi^{(j)}=\frac{1}{r}\delta(x-\xi)\cdot\delta(r-\eta)\cdot\delta_{i1} \qquad \text{(B-1)}$$

subject to the conditions

$$\chi^{(j)}(x, r; \xi, \eta)=0, \qquad \begin{cases} r=b,\ 0\leqslant x\leqslant l; \\ x=(0, l),\ 0\leqslant r\leqslant b, \end{cases} \qquad \text{(B-2)}$$

$$\frac{\partial\chi^{(j)}}{\partial r}(x, 0; \xi, \eta)=0, \qquad \text{(B-3)}$$

$$k_{10}\left(\frac{\partial\chi^{(j)}}{\partial r}\right)_{r=a^-}=k_{20}\left(\frac{\partial\chi^{(j)}}{\partial r}\right)_{r=a^+}, \qquad \text{(B-4)}$$

$$(\chi^{(j)})_{r=a^-}=\sigma_j(\chi^{(j)})_{r=a^+}. \qquad \text{(B-5)}$$

A Fourier sine series for the solution is obtained by taking the finite Fourier transform.

$$\chi^T(\alpha, r; \xi, \eta)=\int_0^l dx\chi(x, r; \xi, \eta)\sin\alpha x,$$

$$\chi(x, r; \xi, \eta)=\frac{2}{l}\sum_{n=0}^{\infty}\chi^T(\alpha_n, r; \xi, \eta),$$

$$\alpha_n\equiv\frac{n\pi}{l}. \qquad \text{(B-6)}$$

which satisfies the conditions (B-2) at $x=(0, l)$. We obtain the equations (dropping the superscript (j)):

$$k_{10}\frac{1}{r}\frac{d}{dr}r\frac{d\chi^T}{dr}+(\mathscr{I}_1^2\bar{\rho}_1(1+\tau)-k_{10}\alpha^2)\chi^T=\sin\alpha\xi\frac{\delta(r-\eta)}{\eta}, \qquad (r<a); \qquad \text{(B-7a)}$$

$$k_{20}\frac{1}{r}\frac{d}{dr}r\frac{d\chi^T}{dr}-k_{20}\alpha^2\chi^T=0, \qquad (r>a). \qquad \text{(B-7b)}$$

For $r>\alpha$, the solution satisfying (A-2) is:

$$\chi^T(\alpha, r)=D_1\left[I_0(\alpha r)-\frac{I_0(\alpha b)}{K_0(\alpha b)}K_0(\alpha r)\right]. \qquad \text{(B-8)}$$

For $0\leqslant r<\eta$, the solution satisfying (A-3) is:

$$\chi^T(\alpha, r)=D_2J_0\left(\frac{r}{l}\epsilon\right), \qquad \text{(B-9)}$$

where

$$\epsilon\equiv\beta^2-(\alpha l)^2,$$
$$\beta^2\equiv\mathscr{I}_1^2\bar{\rho}_1l^2(1+\tau)/k_{10}. \qquad \text{(B-10)}$$

For $\eta<r<\alpha$, the general solution is:

$$\chi^T(\alpha, r)=D_3J_0\left(\frac{r}{l}\epsilon\right)+D_4Y_0\left(\frac{r}{l}\epsilon\right). \qquad \text{(B-11)}$$

The four constants D_i are readily found from conditions (B-4, B-5) at $r=\alpha$, and from jump conditions at $r=\eta$:

$$\chi^T(\alpha, \eta^-)=\chi^T(\alpha, \eta^+),$$
$$\frac{\partial\chi^T}{\partial r}(\alpha, \eta^-)=\frac{\partial\chi^T}{\partial r}(\alpha, \eta^+)-\frac{\sin\alpha\xi}{\eta k_{10}}. \qquad \text{(B-12)}$$

We obtain for the axial value

$$\chi(0, r; \xi, \eta)=\frac{\pi}{lk_{10}}\sum_{n=1}^{\infty}\left[\frac{1}{R_n}J_0\left(\frac{\eta}{l}\epsilon_n\right)+Y_0\left(\frac{\eta}{l}\epsilon\right)\right]\cdot\sin\frac{\pi n\xi}{l}\sin\frac{\pi nx}{l}, \qquad \text{(B-13)}$$

where

$$R_n=-\frac{J_1\left(\frac{a}{l}\epsilon_n\right)C_n^*+\frac{\alpha_nlk_{20}}{\sigma\epsilon k_{10}}J_0\left(\frac{a}{l}\epsilon_n\right)}{Y_1\left(\frac{a}{l}\epsilon_n\right)C_n^*+\frac{\alpha_nlk_{20}}{\sigma\epsilon k_{10}}Y_0\left(\frac{a}{l}\epsilon_n\right)}$$

$$C_n^*=\frac{I_0(a\alpha_n)K_0(b\alpha_n)-I_0(b\alpha_n)K_0(a\alpha_n)}{I_1(a\alpha_n)K_0(b\alpha_n)-I_0(b\alpha_n)K_1(a\alpha_n)}. \qquad \text{(B-14)}$$

All that is required in the text is the integral of this on η. We obtain

$$\int_0^a d_{\eta\eta}\chi^{(j)}(x, 0; \xi, \eta)=\frac{-\pi l}{2k_{10}\beta_j^2}\sum_{n=0}^{\infty} n\phi_n^{(j)} \sin\frac{\pi n\xi}{l}\sin\frac{\pi nx}{l}. \tag{B-15}$$

$$\phi_n^{(j)} \equiv \frac{4\beta_j^2}{\pi n\epsilon_{jn}^2}\left[\frac{1}{J_0\left(\frac{a}{l}\epsilon_{jn}\right)+\frac{\sigma_j\epsilon_{jn}k_{10}}{n\pi k_{20}}J_1\left(\frac{a}{l}\epsilon_{jn}\right)}-1\right]. \tag{B-16}$$

Note that the integral (B–15) is symmetric in (x, ξ). From (A–15), we obtain

$$\begin{aligned} G^{(j)}(x) &\equiv -\bar{\rho}_1\mathcal{J}_1^2(1+\tau_j)\int_0^l d\xi\int_0^a d_{\eta\eta}\chi^{(j)}(x, 0; \xi, \eta) \\ &= -\bar{\rho}_1\mathcal{J}_1^2(1+\tau_j)\int_0^l d\xi\int_0^a d_{\eta\eta}\chi^{(j)}(\xi, 0; x, \eta) \\ &= \sum_{n=1}^{\infty}{}^{*}\phi_n^{(j)}\sin\frac{n\pi x}{l} \end{aligned} \tag{B-17}$$

The Bessel functions occurring in $\phi_n^{(j)}$ are computed from polynomial approximations [9].

7. References

[1] Engen, G. F., A bolometer mount efficiency measurement technique, J. Res. NBS **65C** (Engr. and Instr.) No. 2, 113–124 (1961).

[2] Engen, G. F., A refined X-band microwave microcalorimeter, J. Res. NBS **63C** (Engr. and Instr.) No. 1, 77–82 (1959).

[3] Carlin, H. J., and Sucher, M., Accuracy of bolometric power measurements, Proc. IRE **40,** 1042–1048 (1952).

[4] Weber, E., On microwave power measurements, Elektrotech. Maschinenbau, **71,** 254-259 (1954).

,5. Bleaney, B. (1946), Radio-frequency power measurements by bolometer lamps at centimeter wavelengths, J. Inst. Elec. Engrs. (London) IIIA **93,** 1378–1382 (1946).

[6] Sondheimer, E. H., The mean free path of electrons in metals, Advan. in Phys. **1,** No. 1 (1952).

[7] Holland, L., and Siddall, G., Reactive sputtering and associated plant design, Vacuum **3,** 245 (1953).

[8] Reynolds, F. W. and G. R. Stilwell, Mean free paths of electrons in evaporated metal films of copper and silver, Phys. Rev. **88,** 418 (1952).

[9] Abramowitz, M. and Stegun, I. A. Handbook of mathematical functions, NBS AMS 55 (1964).

(Paper 72C–272)